ELSEVIER

Journal of Organometallic Chemistry 535 (1997) 175–181

Journal of Organometallic Chemistry

Mixed-metal cluster chemistry V [1] Syntheses and X-ray crystal structure of $Cp_2Mo_2Ir_2(\mu_3\text{-}CO)(\mu\text{-}CO)_5(CO)_4$

Nigel T. Lucas [a], Mark G. Humphrey [a,*], David C.R. Hockless [b]

[a] *Department of Chemistry, Australian National University, Canberra, ACT 0200, Australia*
[b] *Research School of Chemistry, Australian National University, Canberra, ACT 0200, Australia*

Received 5 November 1996; accepted 21 December 1996

Abstract

The mixed-metal cluster $Cp_2Mo_2Ir_2(CO)_{10}$ has been synthesized by two procedures, namely reacting $CpMo(CO)_3H$ with $IrCl(CO)_2$(*p*-toluidine) under a CO atmosphere in the presence of zinc (23%), and by combining $[CpMo(CO)_3]^-$ with $IrCl(CO)_2$(*p*-toluidine) (78%). A structural study reveals that, in contrast to the analogous $Cp_2W_2Ir_2(CO)_{10}$, it is a rare example of a tetrahedral cluster with all edges bridged by CO, and that it possesses an unusual 'semi-face-capping' carbonyl ligand. Carbonyl bridging and hence steric crowding increase on proceeding from tungsten to molybdenum, rendering the title complex amongst the most crowded of metal clusters.

Keywords: Molybdenum; Iridium; Carbonyl; Cyclopentadienyl; Cluster; Crystal structure

1. Introduction

Mixed-metal clusters have been of significant interest recently, as their polar metal–metal bonds may give rise to enhanced reactivity compared to that observed with homonuclear clusters. To systematically assess the impact of polar metal–metal bonds on cluster reactivity, one requires access to a specifically substituted isostructural series of clusters in which ligated metal fragments are sequentially replaced by isolobal fragments with different metals. An ideal starting complex is tetrahedral $Ir_4(CO)_{12}$ (**1**), for which comprehensive reactivity data have been reported [2]. Shapley et al. [3], and Churchill and co-workers [4,5] have reported the syntheses and structural characterization of the Group 6–Group 9 mixed-metal clusters $CpWIr_3(CO)_{11}$ (**2**) and $Cp_2W_2Ir_2(CO)_{10}$ (**3**), derived (conceptually) from **1** by stepwise replacement of $Ir(CO)_3$ vertices by $CpW(CO)_2$ units. Introduction of the early transition metal dramatically affects reactivity. For example, the chemistry of clusters **1**–**3** with alkyne ligands has been probed, with the mixed-metal clusters showing greatly enhanced reactivity compared to **1**; the differing chemistry of **2** and **3** has been used to rationalize butane hydrogenolysis over cluster-derived bimetallic catalysts [6–8]. More recently, we have found that phosphine substitution at **2** and **3** proceeds in a stepwise fashion at room temperature [9–11], in contrast to **1** where similar ligand replacement requires refluxing toluene or halide activation to proceed. Subsequent thermolyses of the triphenylphosphine derivatives of **2** afford clusters containing ligand fragments not thus far identified in the tetrairidium system [12]. Base-assisted condensation of **3** affords a heptanuclear cluster with an unprecedented (for transition metals) core geometry [1], whereas base-promoted condensation of **1** afforded hexa-, octa-, nona- and deca-iridium clusters [13–15].

The enhanced reactivity of **2** and **3** compared to **1** (and in some instances their unique behaviour) prompted us to expand this study to embrace the molybdenum analogues. 4d metals form weaker M–M bonds; it may thus be possible to program the cluster core to react at a particular site by weakening specific M–M linkages on replacing tungsten by molybdenum. The synthesis and

* Corresponding author.
[1] For part IV, see Ref. [1].

0022-328X/97/$17.00
PII S0022-328X(97)00032-6

structural characterization of $CpMoIr_3(CO)_{11}$ (**4**) has appeared [16]. The title cluster $Cp_2Mo_2Ir_2(CO)_{10}$ (**5**) has also been prepared previously but in low yield as a minor product in the synthesis of **4** [16]; both **4** and **5** have been utilized as precursors to bimetallic catalysts on an alumina support [17]. However, no spectroscopic data or details on the molecular geometry of $Cp_2Mo_2Ir_2(CO)_{10}$ (**5**) are extant. We report herein syntheses of **5** in useful yields by two procedures, a structural determination of **5**, and comparison of relevant spectroscopic and structural data for complexes **3** and **5**.

2. Results and discussion

2.1. Syntheses and characterization of $Cp_2Mo_2Ir_2(CO)_{10}$ (5)

Cluster **5** is accessible in fair to excellent yield by two synthetic procedures (Scheme 1). Reaction of $CpMo(CO)_3H$ with $IrCl(CO)_2$(*p*-toluidine) and zinc (as reducing agent) affords a mixture of **4** (38%) and **5** (23%). A better yield of **5** (78%) is obtained when $[CpMo(CO)_3]^-$ is reacted with $IrCl(CO)_2$(*p*-toluidine), possibly via the intermediacy of $Cp(CO)_3Mo$–$Ir(CO)_2$(*p*-toluidine) and thence $Cp(CO)_2Mo{\equiv}Ir(CO)_3$, analogous to the mechanistic pathway postulated in the related tungsten system [16]. The solution IR spectrum of **5** in cyclohexane indicates the presence of bridging as well as terminal carbonyl ligands, with the number of bands consistent with the presence of isomers. The ^1H NMR spectrum contains a sharp singlet at about 5 ppm, indicative of two equivalent cyclopentadienyl groups, and suggesting that the isomers observed in the IR spectrum exchange rapidly on the NMR time frame. The mass spectrum contains a molecular ion and consecutive loss of all ten carbonyl ligands; loss of one cyclopentadienyl group becomes competitive with loss of carbonyl upon fragmentation of $[M - 5CO]^+$.

2.2. X-ray structural study of $Cp_2Mo_2Ir_2(CO)_{10}$ (5)

A single crystal X-ray diffraction study of **5** was carried out and confirms the expected molecular composition. Fractional atomic coordinates are given in Table 1 and selected bond lengths and angles displayed in Table 2. Fig. 1 contains an ORTEP plot of **5** showing the molecular structure and atomic labelling scheme.

Table 1
Non-hydrogen atom coordinates and equivalent isotropic displacement parameters for $Cp_2Mo_2Ir_2(CO)_{10}$ (**5**)

Atom	*x*	*y*	*z*	B_{eq}
Ir(1)	0.84490(4)	0.06322(5)	0.12758(4)	2.87(1)
Ir(2)	0.83162(4)	0.06796(5)	0.30399(4)	2.99(1)
Mo(3)	0.68472(8)	0.18694(9)	0.17561(8)	2.50(2)
Mo(4)	0.71335(8)	−0.10390(9)	0.18463(8)	2.64(2)
O(11)	0.893(1)	−0.102(1)	−0.0207(9)	7.3(4)
O(12)	1.0253(8)	−0.016(1)	0.2617(8)	6.0(3)
O(13)	0.6717(7)	0.1028(9)	−0.0250(7)	4.1(3)
O(14)	0.9395(8)	0.3004(9)	0.0743(8)	5.2(3)
O(21)	0.925(1)	0.310(1)	0.3779(9)	7.6(4)
O(22)	0.8773(9)	−0.073(1)	0.4820(7)	5.5(3)
O(23)	0.6504(8)	0.1425(9)	0.3732(7)	4.8(3)
O(31)	0.4869(7)	0.0628(9)	0.1617(8)	4.8(3)
O(41)	0.8911(9)	−0.280(1)	0.277(1)	7.1(4)
O(42)	0.6462(8)	−0.144(1)	0.3677(7)	5.0(3)
C(11)	0.875(1)	−0.041(1)	0.037(1)	4.1(4)
C(12)	0.9475(9)	0.020(1)	0.2389(9)	3.2(3)
C(13)	0.704(1)	0.110(1)	0.047(1)	3.2(3)
C(14)	0.905(1)	0.210(1)	0.095(1)	3.6(3)
C(21)	0.894(1)	0.219(2)	0.351(1)	5.2(5)
C(22)	0.862(1)	−0.020(1)	0.414(1)	3.6(3)
C(23)	0.690(1)	0.137(1)	0.318(1)	3.3(3)
C(31)	0.564(1)	0.095(1)	0.164(1)	3.5(3)
C(41)	0.826(1)	−0.195(1)	0.244(1)	4.4(4)
C(42)	0.672(1)	−0.121(1)	0.301(1)	3.6(3)
C(301)	0.603(1)	0.355(1)	0.100(1)	5.0(4)
C(302)	0.701(1)	0.372(1)	0.095(1)	4.0(4)
C(303)	0.749(1)	0.394(1)	0.184(1)	4.6(4)
C(304)	0.685(1)	0.387(1)	0.242(1)	4.5(4)
C(305)	0.595(1)	0.363(1)	0.187(1)	5.3(5)
C(401)	0.590(1)	−0.138(1)	0.057(1)	4.2(4)
C(402)	0.675(1)	−0.179(1)	0.035(1)	4.7(4)
C(403)	0.712(1)	−0.281(1)	0.092(1)	4.7(4)
C(404)	0.647(1)	−0.299(1)	0.150(1)	4.7(4)
C(405)	0.570(1)	−0.210(1)	0.129(1)	5.1(4)

Cluster **5** possesses an Mo_2Ir_2 pseudotetrahedral core geometry with each molybdenum ligated by one cyclopentadienyl group, each iridium bearing two terminal carbonyl ligands, and six carbonyl ligands in bridging sites completing the coordination geometry; the cluster is thus electron precise with 60 CVE. The Ir(1)–Ir(2) distance (2.6972(9) Å) is similar to those found in clusters **2**–**4** (2.697(1)–2.72(1) Å), and the Mo–Ir parameters (2.838(1)–2.871(1) Å) within the range of those

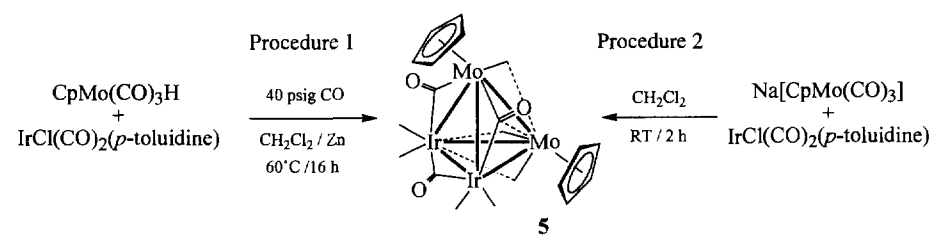

5

Scheme 1. Syntheses of $Cp_2Mo_2Ir_2(CO)_{10}$ (**5**).

observed in **4** (2.835(2)–2.902(2) Å). The Mo–Mo linkage in **5** is long (3.111(1) Å), but not exceptionally so; unsupported Mo–Mo vectors as long as 3.28 Å have been crystallographically confirmed [18]. Four of the carbonyl ligands attached to the iridium atoms (CO11, CO14, CO21, CO22) are 'normal' terminal carbonyls (Ir–CO 1.86(2)–1.90(2) Å, ∠Ir–C–O 176(2)–178(1)°), but all other carbonyl groups interact with more than one metal. Three carbonyl ligands (CO12, CO13, CO23) adopt true bridging geometries about the metal–metal vectors in the Ir(1)Ir(2)Mo(3) plane, the first-mentioned being somewhat asymmetrically disposed (Ir(1)–C(12) 2.06(1) Å, Ir(2)–C(12) 2.14(1) Å), unlike the other two. The final three carbonyl ligands, all bound to molybdenum, adopt semi-bridging geometries. Curtis and coworkers have defined an asymmetry parameter α to evaluate semi-bridging character [19,20], with values of

Table 2
Selected bond lengths (Å) and angles (deg) for $Cp_2Mo_2Ir_2(CO)_{10}$ (**5**)

Ir(1)–Ir(2)	2.6972(9)	Mo(4)–C(402)	2.36(1)
Ir(1)–Mo(3)	2.855(1)	Mo(4)–C(403)	2.33(1)
Ir(1)–Mo(4)	2.838(1)	Mo(4)–C(404)	2.29(1)
Ir(2)–Mo(3)	2.860(1)	Mo(4)–C(405)	2.34(2)
Ir(2)–Mo(4)	2.871(1)	C(11)–O(11)	1.16(2)
Mo(3)–Mo(4)	3.111(1)	C(14)–O(14)	1.14(2)
Ir(1)–C(11)	1.86(2)	C(21)–O(21)	1.11(2)
Ir(1)–C(14)	1.89(2)	C(22)–O(22)	1.15(2)
Ir(2)–C(21)	1.90(2)	C(31)–O(31)	1.15(2)
Ir(2)–C(22)	1.88(2)	C(41)–O(41)	1.18(2)
Mo(3)–C(31)	1.97(1)	C(42)–O(42)	1.16(2)
Mo(4)–C(41)	1.95(2)	C(12)–O(12)	1.17(2)
Mo(4)–C(42)	1.96(2)	C(13)–O(13)	1.09(1)
Ir(1)–C(12)	2.06(1)	C(23)–O(23)	1.09(2)
Ir(2)–C(12)	2.14(1)	C(301)–C(302)	1.43(2)
Ir(1)–C(13)	2.20(1)	C(302)–C(303)	1.41(2)
Mo(3)–C(13)	2.17(2)	C(303)–C(304)	1.39(2)
Ir(2)–C(23)	2.21(2)	C(304)–C(305)	1.41(2)
Mo(3)–C(23)	2.20(2)	C(305)–C(301)	1.35(2)
Mo(3)–C(301)	2.31(1)	C(401)–C(402)	1.35(2)
Mo(3)–C(302)	2.35(2)	C(402)–C(403)	1.42(2)
Mo(3)–C(303)	2.37(2)	C(403)–C(404)	1.40(2)
Mo(3)–C(304)	2.34(1)	C(404)–C(405)	1.44(2)
Mo(3)–C(305)	2.29(1)	C(405)–C(401)	1.40(2)
Mo(4)–C(401)	2.37(1)		
Ir(2)–Ir(1)–Mo(3)	61.93(3)	Ir(2)–C(23)–Mo(3)	80.8(5)
Ir(2)–Ir(1)–Mo(4)	62.41(3)	Ir(1)–C(11)–O(11)	178(1)
Mo(3)–Ir(1)–Mo(4)	66.23(3)	Ir(1)–C(14)–O(14)	178(1)
Ir(1)–Ir(2)–Mo(3)	61.75(3)	Ir(2)–C(21)–O(21)	176(2)
Ir(1)–Ir(2)–Mo(4)	61.20(3)	Ir(2)–C(22)–O(22)	178(1)
Mo(3)–Ir(2)–Mo(4)	65.75(3)	Mo(3)–C(31)–O(31)	167(1)
Ir(1)–Mo(3)–Ir(2)	56.32(3)	Mo(4)–C(41)–O(41)	174(1)
Ir(1)–Mo(3)–Mo(4)	56.62(3)	Mo(4)–C(42)–O(42)	173(1)
Ir(2)–Mo(3)–Mo(4)	57.29(3)	Ir(1)–C(12)–O(12)	144(1)
Ir(1)–Mo(4)–Ir(2)	56.38(3)	Ir(2)–C(12)–O(12)	136(1)
Ir(1)–Mo(4)–Mo(3)	57.15(3)	Ir(1)–C(13)–O(13)	135(1)
Ir(2)–Mo(4)–Mo(3)	56.96(3)	Mo(3)–C(13)–O(13)	143(1)
Ir(1)–C(12)–Ir(2)	79.9(5)	Ir(2)–C(23)–O(23)	136(1)
Ir(1)–C(13)–Mo(3)	81.5(5)	Mo(3)–C(23)–O(23)	143(1)

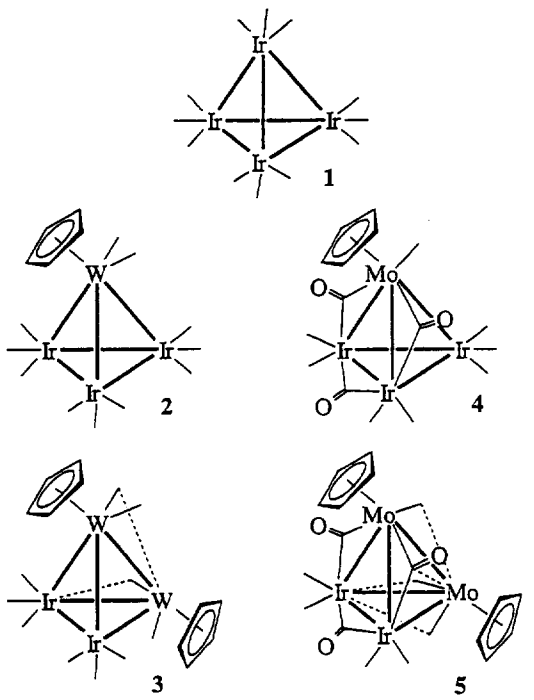

Fig. 1.

α between 0.1 and 0.6 corresponding to semi-bridging. For these carbonyl groups, Mo(3)–C(31) · · · Mo(4) has $\alpha = 0.51$, Mo(4)–C(41) · · · Ir(2) has $\alpha = 0.50$, and Mo(4)–C(42) · · · Ir(2) has $\alpha = 0.55$, all well within the semi-bridging domain. In addition, CO13 is tilted toward Mo(4) (the dihedral angle of Mo(3)C(13)Ir(1) with the Mo(3)Ir(1)Ir(2) plane is 21.40°, whereas the corresponding dihedral angles for the other bridging carbonyls (Mo(3)C(23)Ir(2) 12.96°, Ir(1)C(12)Ir(2) 13.28°) are significantly smaller); the Mo(4) · · · C(13) distance of 3.06(1) Å affords asymmetry parameters of $\alpha = 0.39$ with Ir(1) and $\alpha = 0.41$ with Mo(3), suggesting that CO(13) is an unusual 'semi-face-capping' carbonyl ligand (other molybdenum-containing examples are extant: see Refs. [21,22]). Because of these semi-bridging interactions, all metal–metal bonds in **5** have bridging carbonyls. Very few clusters have been structurally characterized with six or more bridging carbonyls [22–30] and of these only $Ni_4(CO)_6(PMe_3)_4$ [23,24], $Ni_4(CO)_6[P(CH_2CH_2CN)_3]_4$ [30] and $Pd_4(CO)_6(PBu^n_3)_4$ [25] possess tetrahedral core geometries.

2.3. Discussion

It was pointed out by Churchill et al. that **3** is amongst the most crowded of tetranuclear clusters [5]; assuming that Cp occupies 2.5 coordination sites, it is an example of an $M_4(CO)_{15}$ cluster (with no examples of $M_4(CO)_{16}$ thus far structurally confirmed). A comparison of spectroscopic and crystallographic data from **3** with those from **5** is therefore of obvious interest, and

is presented in Table 3, with atoms in **3** relabelled for consistency.

Fig. 2 shows the molecular structure and atomic labelling scheme for $Cp_2Mo_2Ir_2(CO)_{10}$ (**5**). Thermal envelopes of 50% probability are shown for the non-hydrogen atoms; hydrogen atoms have arbitrary radii of 0.1 Å.

The bridging carbonyl bands in the IR spectra increase in number and decrease in energy in proceeding from **3** to **5** (i.e. to the lighter metal). Both **3** and **5** fragment similarly in the MS, with a less intense molecular ion and more intense fragment ions $[M - nCO]^+$, $n > 4$, being observed for the cluster with the lighter metal, possibly indicative of enhanced reactivity. Core bond distances for **3** and **5** are comparable with the exception of Ir(2)–M(3) and M(3)–M(4), both substantially longer for **5**. It is in the carbonyl disposition about the cluster cores where the greatest disparity between **3** and **5** lies. The presence of bridging carbonyls about the Ir(1)Ir(2)M(3) plane in **5**, but not **3**, does not lead to a decrease in metal–metal bond lengths for **5** compared with **3** (in fact there is a substantial elongation of the Ir(2)–Mo(3) vector). Semi-bridging interactions Ir(2) · · · C(42) and M(4) · · · C(31) are both 0.2 Å longer in **5** than in **3**, consistent with **5** being the more sterically encumbered cluster. Angle Ir(2) · · · C(42)–M(4) is significantly more acute in **5** than in **3**, but this carbonyl is semi-bridging in **3** and semi-face-capping in **5**. Ignoring all semi-bridging and semi-face-capping interactions, all cluster metal atoms have 18 electron counts. Semi-bridging CO(31) redirects electron density from Mo(3) to Mo(4), and semi-face-capping CO(13) transfers charge from Mo(3) and Ir(1) to Mo(4). Similarly, semi-bridging CO(41) and CO(42) transfers electron density from Mo(4) to Ir(2). The net effect is to make Mo(3) slightly electron deficient and Ir(2) slightly electron rich. In **3**, semi-bridging W(3)–C(31) · · · W(4) and W(4)–C(42) · · · Ir(2) were compensated by a short Ir(2)–W(3) linkage presumed to result from direct electron transfer from Ir(2) to W(3). This effect is not observed in **5**, with any charge asymmetry resulting from bridging carbonyls uncompensated by Ir(2) → Mo(3) electron transfer. As all metals have 18 valence electron counts, the semi-bridging interactions in **3** and

Table 3
Selected spectroscopic and crystallographic data for $Cp_2W_2Ir_2(CO)_{10}$ (**3**) and $Cp_2Mo_2Ir_2(CO)_{10}$ (**5**)

	$Cp_2W_2Ir_2(CO)_{10}$ (**3**)	$Cp_2Mo_2Ir_2(CO)_{10}$ (**5**)
IR (C_6H_{12})		
ν(CO) (cm^{-1})	2067 s	2063 m
	2032 vs	2046 w
	2010 vs	2034 vs
	2000 s	1998 w
	1987 m	1990 w
	1968 w	1977 w
	1926 m	1940 w
	1896 w	1927 w
	1833 w	1887 w
		1866 w
		1768 w
^{1}H NMR (δ $CDCl_3$)		
(s, 10H, Cp)	5.33	4.98
MS m/z (rel. intensity)		
$[M]^+$	1162 (25)	986 (13)
$[M-CO]^+$	1134 (17)	958 (31)
$[M-2CO]^+$	1106 (62)	930 (78)
$[M-3CO]^+$	1078 (100)	902 (81)
$[M-4CO]^+$	1050 (88)	874 (48)
$[M-5CO]^+$	1022 (78)	846 (100)
$[M-6CO]^+$	994 (75)	818 (89)
$[M-7CO]^+$	966 (63)	790 (75)
$[M-5CO-Cp]^+$	957 (13)	781 (37)
$[M-8CO]^+$	938 (37)	762 (68)
$[M-6CO-Cp]^+$	929 (17)	753 (52)
$[M-9CO]^+$	910 (29)	734 (63)
$[M-7CO-Cp]^+$	901 (15)	725 (44)
$[M-10CO]^+$	882 (27)	706 (50)
Metal–metal bond lengths		
	M = W	M = Mo
Ir(1)–Ir(2)	2.722(1)	2.6972(9)
Ir(1)–M(3)	2.833(1)	2.855(1)
Ir(1)–M(4)	2.847(1)	2.838(1)
Ir(2)–M(3)	2.796(1)	2.860(1)
Ir(2)–M(4)	2.863(1)	2.871(1)
M(3)–M(4)	2.991(1)	3.111(1)
Short metal–carbonyl carbon contacts		
Ir(2) · · · C(41)		2.93(1)
Ir(2) · · · C(42)	2.835(14)	3.04(1)
M(4) · · · C(13)		3.06(1)
M(4) · · · C(31)	2.794(14)	2.98(1)

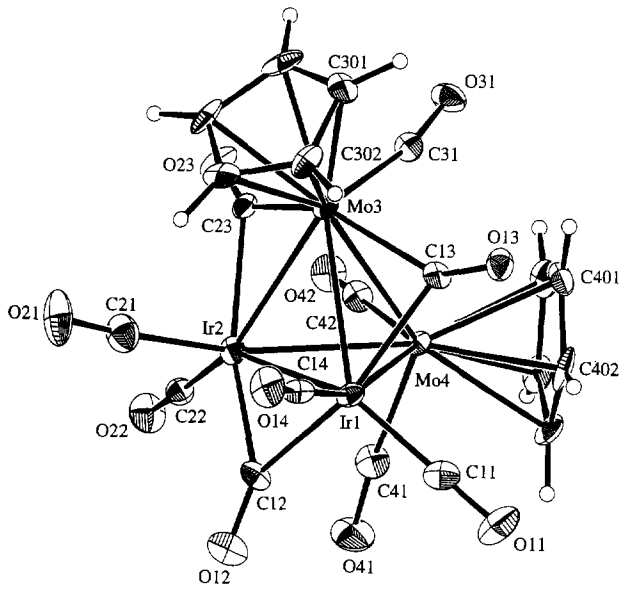

Fig. 2. Shows the molecular structure and atomic labelling scheme for $Cp_2Mo_2Ir_2(CO)_{10}$ (**5**). Thermal envelopes of 50% probability are shown for the non-hydrogen atoms; hydrogen atoms have arbitrary radii of 0.1 Å.

5 serve only to relieve steric stress in the clusters; the larger number of semi-bridging interactions and uncompensated charge asymmetry in 5 suggest that steric pressure is significantly greater for 5.

The proclivity of carbonyls to adopt bridging geometries in clusters of the lighter metals leads then in the present case to an example even more crowded than 3, reflected in compensating bond lengthening. Cluster $Cp_2Mo_2Co_2(\mu\text{-}CO)_3(CO)_7$, related to 5 by replacement of Ir by the smaller Co, may have been expected to be even more sterically hindered than 5, but no semi-bridging interactions have been found [31]. With respect to the plane of bridging carbonyls, the cyclopentadienyl ligands occupy apical, radial sites in the cobalt example, unlike in 5 where an apical, axial geometry is observed. It is well-established that the radial substitution sites are less sterically hindered than the axial sites [10]. It seems therefore that the title cluster 5 is the most sterically encumbered example from this mixed-metal system, but the reason for the differing site preference of the cyclopentadienyl ligand is not clear at this stage.

The role of steric factors in mixed-metal tetranuclear clusters is of current interest [32]. The steric congestion at the title cluster may be expected to influence its chemistry significantly, an aspect we are currently probing. For example, 3 adds two equivalents of PPh_3 whereas 5 adds one only [33], a result readily explicable on steric grounds. Further comparative reactivity studies are currently under way.

3. Experimental details

3.1. General conditions

Reactions were performed under either an atmosphere of argon (high-purity, CIG) or carbon monoxide (high-purity, CIG) although no special precautions were taken to exclude air during work-up. The reaction solvent CH_2Cl_2 was dried by distillation over CaH_2 under a nitrogen atmosphere. Petroleum spirit refers to a petroleum fraction of boiling range 60–80 °C. The products were purified by thin-layer chromatography on $20 \times 20\,cm^2$ glass plates coated with Merck GF_{254} silica gel (0.5 mm). Literature procedures were used to synthesize $CpMo(CO)_3H$ [34], $IrCl(CO)_2$(*p*-toluidine) [35] and $Na[CpMo(CO)_3]$ [36].

3.2. Instruments

Infrared spectra were recorded on a Perkin–Elmer System 2000 FT-IR with CaF_2 optics. ^1H NMR spectra were recorded in $CDCl_3$ using a Varian Gemini-300 (at 300 MHz) and are referenced to residual $CHCl_3$ (7.24 ppm). Mass spectra were recorded using a VG ZAB 2SEQ instrument (30 kV Cs^+ ions, current 1 mA, accelerating potential 8 kV, 3-nitrobenzyl alcohol matrix) at the Research School of Chemistry, Australian National University. Microanalyses were carried out by the Microanalysis Service Unit in the Research School of Chemistry, Australian National University.

3.3. Preparation of $Cp_2Mo_2Ir_2(CO)_{10}$ (1)

3.3.1. Procedure 1

A dichloromethane solution (150 ml) of freshly prepared $CpMo(CO)_3H$ (380 mg, 1.54 mmol) was added to $IrCl(CO)_2$(*p*-toluidine) (210 mg, 0.54 mmol) and acid-washed granular zinc (ca. 1.0 g) in an argon-filled 250 ml glass pressure bottle. After attaching the pressure head, the bottle was pressured to 40 psig with carbon monoxide and placed in an oil bath at 60 °C for 16 h, over which period the reaction mixture was stirred. The oil bath was cooled to room temperature, the glass pressure bottle vented, and 5 ml of CCl_4 added to the reaction mixture to convert the remaining $CpMo(CO)_3H$ to $CpMo(CO)_3Cl$ for easier work-up. The reaction mixture was stirred for 15 min under an argon atmosphere, and then filtered and evaporated to dryness on a rotary evaporator. The red solid residue was extracted with dichloromethane (8–10 ml) and the resultant solution applied to preparative TLC plates. Elution with dichloromethane–petroleum spirit (2:5) gave bands of pink $[CpMo(CO)_3]_2$ ($R_f = 0.54$, trace), orange $CpMoIr_3(CO)_{11}$ ($R_f = 0.38$), brown $Cp_2Mo_2Ir_2(CO)_{10}$ ($R_f = 0.14$) and orange $CpMo(CO)_3Cl$ ($R_f = 0.08$). The material in the orange band ($R_f = 0.38$) of $CpMoIr_3(CO)_{11}$ (4) was crystallized from dichloromethane–methanol by liquid diffusion at 3 °C (53 mg, 38%) and identified by comparison of its IR and ^1H NMR spectra with literature values [16]. The brown band was extracted with dichloromethane and the resultant solution evaporated to dryness. The crude product was recrystallized from dichloromethane–methanol by liquid diffusion at 3 °C over 24 h to afford red-brown crystalline $Cp_2Mo_2Ir_2(CO)_{10}$ (5) (60 mg, 0.061 mmol, 23%). Anal. Found: C, 24.02; H, 0.91%. $C_{20}H_{10}Ir_2Mo_2O_{10}$ calcd.: C, 24.35; H, 1.02%. The orange band ($R_f = 0.08$) of $CpMo(CO)_3Cl$ (100 mg, 0.36 mmol, 23%) was identified by comparison of its IR and ^1H NMR with literature values [37].

3.3.2. Procedure 2

Using the procedure of Manning et al. [36], $Na[CpMo(CO)_3]$ was prepared from Na (86 mg, 3.7 mmol), cyclopentadiene (0.85 ml, 802 mg, 12.1 mmol) and $Mo(CO)_6$ (983 mg, 3.7 mmol). $IrCl(CO)_2$(*p*-toluidine) (130 mg, 0.33 mmol) and dry dichloromethane (30 ml) were added in situ to the crude solid $Na[CpMo(CO)_3]$ and the mixture stirred at room temperature for 2 h. The solvent was removed from the reaction mixture by rotary evaporation, and the red-

brown residue dissolved in dichloromethane (3–4 ml) and applied to preparative TLC plates. Elution with dichloromethane–petroleum spirit (2:5) gave two bands. The contents of the first band were identified by solution IR as $CpMoIr_3(CO)_{11}$ (**4**) (trace). The second band contained the major product which was identified by IR, ^1H NMR and MS as $Cp_2Mo_2Ir_2(CO)_{10}$ (**5**) (128 mg, 0.13 mmol, 78%).

3.4. X-ray structure determination

3.4.1. General conditions

Crystals of **5** suitable for diffraction analyses were grown by slow diffusion of ethanol into dichloromethane at 3 °C. Data were collected on a Rigaku AFC6R diffractometer with a 12 kW rotating anode generator utilizing graphite monochromated Cu Kα radiation (λ = 1.54178 Å; ω–2θ scan mode, $2\theta_{max}$ 120.1°). A unique diffractometer data set ($T \approx 296$ K) was obtained, yielding 3543 independent reflections, 2807 of these with $I \geq 3\sigma(I)$ being considered 'observed' and used in the full matrix least squares refinement after application of a face indexed analytical absorption correction. The data were also corrected for Lorentz and polarization effects, and secondary extinction. The structure was solved by direct methods and expanded using Fourier techniques. The non-hydrogen atoms were refined anisotropically. Hydrogen atoms were included at calculated positions but not refined. Conventional residuals R, R_w on $|F|$ at convergence were 0.038, 0.043, the weighting function $w = 1/\sigma^2(F_o) = [\sigma_c^2(F_o) + (p^2/4)F_o^2]^{-1}$ ($\sigma_c^2(F_o)$ = e.s.d. based on counting statistics, $p = 0.0080$ determined experimentally from standard reflections) being employed. Computation used the teXsan package [38]. Pertinent results are given in the figures and tables. Tables of hydrogen atom coordinates and thermal parameters and complete lists of bond lengths and angles for non-hydrogen atoms have been deposited at the Cambridge Crystallographic Data Centre.

3.4.2. Crystal data

$C_{20}H_{10}Ir_2Mo_2O_{10}$, $M = 986.61$. Monoclinic, space group $P2_1/c$ (No. 14), $a = 14.330(4)$, $b = 10.604(2)$, $c = 15.041(4)$ Å, $\beta = 101.15(2)°$, $V = 2242.6(8)$ Å^3, $Z = 4$. $D_{calc} = 2.922$ g cm^{-3}; $F(000) = 1792$. $\mu_{Cu} = 313.65$ cm^{-1}; specimen: 0.36 × 0.04 × 0.01 mm^3; $T_{min,max} = 0.245, 0.732$.

Acknowledgements

We thank the Australian Research Council for support of this work, Johnson-Matthey Technology Centre for a generous loan of iridium salts, and Professor B.K. Nicholson (Waikato University, New Zealand) for helpful discussions. MGH holds an ARC Australian Research Fellowship and NTL holds an RSC Honours Year Scholarship.

References

[1] S.M. Waterman, M.G. Humphrey, D.C.R. Hockless, Organometallics 15 (1996) 1745.
[2] C. Barnes, in: G. Wilkinson, F.G.A. Stone, E.W. Abel (Eds.), Comprehensive Organometallic Chemistry II, vol. 8, Pergamon, Oxford, 1995, p. 490.
[3] J.R. Shapley, S.J. Hardwick, D.S. Foose, G.D. Stucky, J. Am. Chem. Soc. 103 (1981) 7383.
[4] M.R. Churchill, J.P. Hutchinson, Inorg. Chem. 20 (1981) 4112.
[5] M.R. Churchill, C. Bueno, J.P. Hutchinson, Inorg. Chem. 21 (1982) 1359.
[6] J.R. Shapley, M.G. Humphrey, C.H. McAteer, in: S.L. Suib, M. Davis (Eds.), ACS Symposium Series, vol. 517, Selectivity in Catalysis, American Chemical Society, New York, 1993, p. 127.
[7] J.R. Shapley, C.H. McAteer, M.R. Churchill, L.V. Biondi, Organometallics 3 (1984) 1595.
[8] M.G. Humphrey, C.H. McAteer, S.R. Wilson, J.R. Shapley, in preparation.
[9] J. Lee, M.G. Humphrey, D.C.R. Hockless, B.W. Skelton, A.H. White, Organometallics 12 (1993) 3468.
[10] S.M. Waterman, M.G. Humphrey, V. Tolhurst, B.W. Skelton, A.H. White, D.C.R. Hockless, Organometallics 15 (1996) 934.
[11] J. Lee, S.M. Waterman, M.G. Humphrey, D.C.R. Hockless, unpublished results.
[12] S.M. Waterman, V.-A. Tolhurst, M.G. Humphrey, B.W. Skelton, A.H. White, J. Organomet. Chem. 515 (1996) 89.
[13] F. Demartin, M. Manassero, M. Sansoni, L. Garlaschelli, S. Martinengo, F. Canziani, J. Chem. Soc. Chem. Commun. (1980) 903.
[14] R. Della Pergola, F. Cea, L. Garlaschelli, N. Masciocchi, M. Sansoni, J. Chem. Soc. Dalton Trans. (1994) 1501.
[15] F. Demartin, M. Manassero, M. Sansoni, L. Garlaschelli, C. Raimond, S. Martinengo, F. Canziani, J. Chem. Soc. Chem. Commun. (1981) 528.
[16] M.R. Churchill, Y. Li, J.R. Shapley, D.S. Foose, W.S. Uchiyama, J. Organomet. Chem. 312 (1986) 121.
[17] J.R. Shapley, W.S. Uchiyama, R.A. Scott, J. Phys. Chem. 94 (1990) 1190.
[18] W. Clegg, N.A. Compton, R.J. Errington, N.C. Norman, Acta Crystallogr. Sect. C: 44 (1988) 568.
[19] M.D. Curtis, W.M. Butler, J. Organomet. Chem. 155 (1978) 131.
[20] R.J. Klingler, W.M. Butler, M.D. Curtis, J. Am. Chem. Soc. 100 (1978) 5034.
[21] P. Braunstein, J.-M. Jud, A. Tiripicchio, M. Tiripicchio-Camellini, E. Sappa, Angew. Chem. Int. Ed. Engl. 21 (1982) 307.
[22] R. Bender, P. Braunstein, J.-M. Jud, Y. Dusausoy, Inorg. Chem. 23 (1984) 4489.
[23] M. Bochmann, I. Hawkins, M.B. Hursthouse, R.L. Short, J. Organomet. Chem. 332 (1987) 361.
[24] M. Bochmann, I. Hawkins, L.J. Yellowlees, M.B. Hursthouse, R.L. Short, Polyhedron 8 (1989) 1351.
[25] E.G. Mednikov, N.K. Eremenko, S.P. Gubin, Y.L. Slovokhotov, Y.T. Struchkov, J. Organomet. Chem. 239 (1982) 401.
[26] V.G. Albano, P.L. Bellon, G. Ciani, J. Chem. Soc. Dalton Trans. (1988) 1103.
[27] V.G. Albano, P.L. Bellon, G.F. Ciani, J. Chem. Soc. D: (1969) 1024.
[28] A. Fumagalli, G. Longoni, P. Chini, A. Albinati, S. Brückner, J. Organomet. Chem. 202 (1980) 329.

[29] R. Goddard, P.W. Jolly, C. Krüger, K. Schick, G. Wilke, Organometallics 1 (1982) 1709.
[30] M.J. Bennett, F.A. Cotton, B.H.C. Winquist, J. Am. Chem. Soc. 89 (1967) 5766.
[31] V.S. Kaganovich, Y.L. Slovokhotov, A.V. Mironov, Y.T. Struchkov, M.I. Rybinskaya, J. Organomet. Chem. 372 (1989) 339.
[32] P. Braunstein, C. de Méric de Bellefon, S.-E. Bouaoud, D. Grandjean, J.-F. Halet, J.-Y. Saillard, J. Am. Chem. Soc. 113 (1991) 5282.
[33] N.T. Lucas, I.R. Whittall, M.G. Humphrey, D.C.R. Hockless, P.C. Healy, M.L. Williams, in preparation.
[34] S.P. Nolan, C.D. Hoff, Organomet. Synth. 4 (1988) 58.
[35] U. Klabunde, Inorg. Synth. 15 (1974) 82.
[36] A.R. Manning, P. Hackett, R. Birdwhistell, P. Soye, Inorg. Synth. 28 (1990) 148.
[37] T.S. Piper, G. Wilkinson, J. Inorg. Nucl. Chem. 3 (1956) 104.
[38] teXsan, Single Crystal Structure Analysis Software, version 1.6c, 1993 (Molecular Structure Corporation, The Woodlands, TX).